Optics & Laser Technology 68 (2015) 36–40

Contents lists available at ScienceDirect

Optics & Laser Technology

journal homepage: www.elsevier.com/locate/optlastec

Diode-pumped acousto-optical Q-switched 912 nm $Nd:GdVO_4$ laser and extra-cavity frequency-doubling of 456 nm deep-blue light emission

F. Chen [a,b,*], X. Yu [b], K. Zhang [a], Y. He [a], C.B. Zheng [a], C.R. Wang [a], J. Guo [a]

[a] *State Key Laboratory of Laser Interaction with Matter, Changchun Institute of Optics, Fine Mechanics and Physics, Chinese Academy of Sciences, Changchun 130033, China*

[b] *National Key Laboratory of Science and Technology on Tunable Laser, Harbin Institute of Technology, Harbin 150080, China*

ARTICLE INFO

Article history:
Received 9 August 2014
Received in revised form
6 November 2014
Accepted 6 November 2014
Available online 24 November 2014

Keywords:
Diode-pumped laser
912 nm Laser
456 nm Deep-blue light

ABSTRACT

In this paper, a diode-pumped acousto-optical (A-O) Q-switched 912 nm $Nd:GdVO_4$ laser and pulsed 456 nm deep-blue light emission by extra-cavity frequency-doubling are demonstrated. To compensate the serious thermal-lensing effect in laser crystal, a compact unstable resonator is used. At an incident pump power of 49.5 W, a maximum average output power of 2.3 W 912 nm laser is obtained at 10 kHz, corresponding to an optical conversion efficiency of 4.6% and a slope efficiency of 9.2%. Minimum pulse width of 20 ns and maximum peak power of 10.5 kW 912 nm laser are achieved at a pump power of 45.3 W. Using a BiBO crystal as the frequency-doubler, maximum average output power of 623 mW 456 nm deep-blue light is obtained at 10 kHz, with a pulse width of 21.3 ns and a peak power of 2.3 kW. Moreover, stable operating repetition rate of 912 nm laser and 456 nm deep-blue light is up to 100 kHz.

1. Introduction

Diode-pumped quasi-three-level Nd-lasers emitting around 900 nm have many applications such as water vapor lidars and differential absorption lidars (DIALs) for ozone measurements, and some of these lasers also can be used as pump sources for Yb-doped crystals or fibers [1–5]. By using frequency-doubling technology, blue light can be generated efficiently, which has numerous applications ranging from biological and medical diagnostics, high-density optical data storage, color displays to underwater detection and communication [6–10]. Considering the application in remote sensing, pulsed laser is extremely useful, especially high-repetition-rate laser with high-peak-power is in demand for improving the speed and distance in transmission.

Since the first report on diode-pumping continuous-wave (cw) 946 nm Nd:YAG laser by Fan in 1987, much attention was paid on improving the performance of quasi-three-level Nd^{3+}-doped lasers, such as 946 nm Nd:YAG laser, 912 nm $Nd:GdVO_4$ laser, 914 nm $Nd:YVO_4$ laser, 916 nm $Nd:LuVO_4$ laser and so on [11–16]. The $Nd:GdVO_4$ crystal is expected to be a high performance laser medium and is especially suitable for high-power 912 nm laser operation. This is partially due to its high absorption at 808 nm pumping laser and large stimulated emission cross-section at 912 nm oscillating laser (6.6×10^{-20} cm^2). Furthermore, uni-axial crystal structure of $Nd:GdVO_4$ is convenient for obtaining the single polarization laser, which is good for the frequency conversion of quasi-phase match. In the past few years, cw $Nd:GdVO_4$ laser (at the fundamental wavelength of 912 nm laser and the 456 nm deep-blue light) was investigated [17–24]. However, just few pulsed experiments were carried out. In 2010, a passively Q-switched 912 nm $Nd:GdVO_4/Cr^{4+}$:YAG laser and intra-cavity frequency doubling of 456 nm light emission were demonstrated [25,26]. Using a linear cavity, average output power of 2.6 W 912 nm laser was achieved with a pulse width of 10.5 ns and the repetition rate ~81.6 kHz. Using a V-type cavity, 2.8 W 912 nm laser was achieved, and the pulse width and the repetition rate were ~40.5 ns and ~76.6 kHz, respectively. 1.2 W 456 nm pulsed deep-blue light was obtained at a repetition rate ~42.7 kHz. Stable passive mode-locking 912 nm $Nd:GdVO_4$ laser was also demonstrated [27,28]. With a four-mirror-folded cavity and a semiconductor saturable absorber mirror, 6.5 ps laser pulses at 178 MHz were obtained by Xu et al., and the total output power was 128 mW. Using a Z-type cavity with Cr^{4+}:YAG crystals as the intra-cavity saturable absorber, as much as 2.0 W 912 nm laser was produced, the repetition rates of the Q-switched envelope and the mode-locking pulse were ~224 kHz and ~160 MHz, respectively. For the A-O Q-switched mode, pulse width of 20 ns and peak power of 7.1 kW 912 nm laser at 10 kHz were obtained, and pulsed 456 nm light emission with a pulse duration of 140 ns and

* Corresponding author at: State Key Laboratory of Laser Interaction with Matter, Changchun Institute of Optics, Fine Mechanics and Physics, Chinese Academy of Sciences, Changchun 130033, China.
E-mail address: feichenny@126.com (F. Chen).

http://dx.doi.org/10.1016/j.optlastec.2014.11.007

a peak power of 315 W at 10 kHz was also obtained [29,30]. It can be seen that the laser cavity length is too long using intra-cavity frequency-doubling, and extra loss is introduced by inserting the nonlinear crystal. Laser pulses showing wide pulse duration and therefore low peak power could be obtained at high-repetition-rate operation. Some above problems can be avoided by using extra-cavity frequency-doubling.

In this paper, diode-pumped A-O Q-switched 912 nm $Nd:GdVO_4$ laser and extra-cavity frequency-doubling of 456 nm deep-blue light emission were reported. Using a compact thermal-compensating laser cavity, 2.3 W 912 nm laser was obtained at 10 kHz, and minimum pulse width of 20 ns and the highest peak power of 10.5 kW were achieved. Maximum average output power of 623 mW 456 nm deep-blue light is obtained at 10 kHz, with a pulse width of 21.3 ns and a peak power of 2.3 kW. The stable operating repetition rate can be extended to 100 kHz.

2. Experimental setup

The experimental setup of diode-end-pumping A-O Q-switched 912 nm $Nd:GdVO_4$ laser and 456 nm deep-blue light by extra-cavity frequency-doubling is shown in Fig. 1. The pump source is a high brightness fiber-coupled laser diode (HLU110F400, LIMO), which delivers a maximum output power of 110 W at 808 nm from the end of a fiber with 400 μm core in diameter and a N.A. of 0.22. The pump beam is coupled into the gain medium by a coupling optics, which consists of two identical plano-convex lenses with a coupling efficiency of 98%. A conventional $Nd:GdVO_4$ crystal with a doping-concentration of 0.1 at% and the dimensions of $3\times3\times6\ mm^3$ is employed as a gain medium, for low doping concentration and short length crystals can minimize the re-absorption loss, up-conversion, concentration quenching and the amplified spontaneous emission [31,32]. The crystal wrapped with a 0.05 mm thick indium foil is mounted in a copper micro-channel heat sink, and is cooled by water at a temperature of 8 ± 0.1 °C. To prevent the more efficient four-level transitions at 1064 nm and 1342 nm, both sides of the crystal are coated for high transmission (HT) at 912 nm ($T>99.8\%$) and 808 nm ($T>99\%$),while antireflection (AR) coatings at 1064 nm ($R<1\%$) and 1342 nm ($R<2\%$) are considered as well. Experiments are carried out with a compact thermal-compensating laser cavity, which is built by an aspheric plano-convex input mirror M_1 and a plane–plane output mirror M_2. M_1 has AR coating at 808 nm ($R<10\%$) and high reflection (HR) coating at 912 nm ($R>99.8\%$), and M_2 is HT coating at 1064 nm and 1342 nm, and partially at 912 nm. A 20-mm-long A-O Q-switch (Gooch&Housego) is inserted into the laser cavity to obtain short laser pulse. In view of the advantages of large nonlinear coefficient and high laser damage threshold, a BiBO crystal with the dimensions of $3\times3\times15\ mm^3$ is employed as the frequency-doubler. The crystal is cut for type-I critical-phase-matching condition ($\theta=159.5°$, $\varphi=90°$) and installed in a copper holder, whose temperature is precisely controlled by a thermal-electric-cooler with 0.1 °C accuracy. Both facets of the BiBO are well polished and AR coated at 456 nm and 912 nm. The dichroic mirror M_3 is coated 45° HR at 912 nm and 45° AR at 456 nm. M_4 is coated HR at 912 nm and 456 nm. M_5 is coated with 45° HR at 456 nm. D_1 and D_2 are two pinholes with high damage threshold. D_1 is used to restrict the high-order mode oscillation on one hand, and to protect the Q-switch from breakage by the unabsorbed pump laser on the other hand. D_2 is used to prevent the backward 912 nm laser after frequency-doubling from entering the cavity. The Q-switched pulses are recorded by a digital oscilloscope (DPO 7104, Tektronix Inc.) and a fast photodiode (DET 210, Thorlabs Inc.) with a rising time of less than 1 ns. Laser spectra is measured by a fiber spectrometer (HR4000, Ocean Optics Inc.), and output power is recorded by a laser power meter PM30 (PM30, Coherent Inc.).

3. Experimental results and discussion

3.1. Thermal-compensation analysis

Before the pulsed laser is investigated, cw 912 nm laser performance is tested. As a result, the highest output power of 16.2 W 912 nm laser is obtained at an incident pump power of 67.0 W. However, it is found that the thermal effect in the crystal is significantly serious, and the output power is falling evidently as the cavity is lengthening. For Q-switched laser operation, the cavity length should be increased from 20 mm to 45 mm because an A-O Q-switch is inserted.

During the cw laser operation using a plano–plano cavity, the thermal focal length in the crystal is measured employing an interference stripe method [33]. As shown in Fig. 2, the focal length of the laser crystal thermally induced lens reduces with the increase of the incident pump power. When the pump power is higher than 20 W, it is shorter than 50 mm. At a pump power of 49.5 W, it is measured to be 16.8 mm. Therefore, to realize a stable pulsed laser operation, the thermal-lensing should be compensated.

Replacing M_1 with plano-convex mirrors, unstable cavities are built. When the pump power is lower, the thermal effect is not serious, then the cavity is unstable and has no laser outputs. As pump power is increased, the thermal focal length becomes shorter, and the convex-plano cavity becomes stable and the laser is oscillating. When the thermal deformation on the crystal surface is compensated optimally, the G-parameter of the cavity is near that of a plano–plano cavity. Therefore, the cavity can be lengthened and operated stably after compensation. Moreover, the mode volume is increased and the beam quality is improved using the plano-convex cavity. However, the thermal focal length is changing with pump power, so there is an optimal curvature of M_1 (R_1) at different pump powers. According to the theory of ABCD matrix, the optimum R_1 versus the incident pump power is shown in Fig. 3, it can be seen that the optimum R_1 is greater than -50 mm when the pump power is higher than 30 W. In experiments, it is difficult to change the R_1 real-time with the change of pump power, so the optimal compensation region using a fixed R_1 should be estimated. Mode-matching between the oscillating beam and the pump beam is considered as a criterion for estimating the

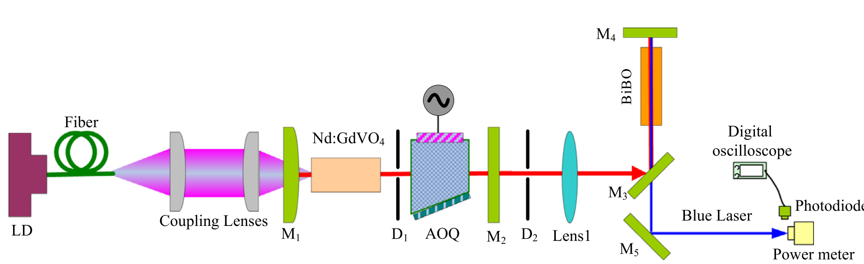

Fig. 1. Schematic of the experimental setup.

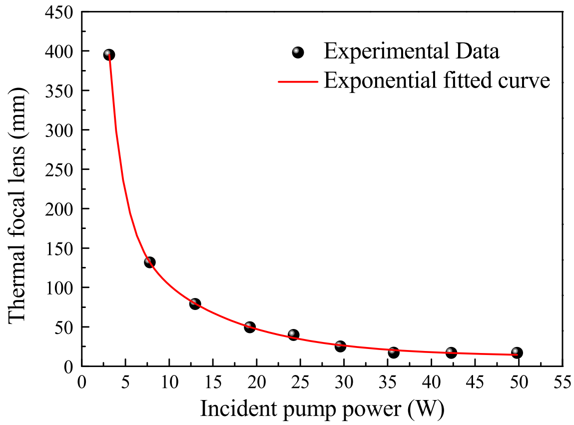

Fig. 2. Thermal focal length versus incident pump power.

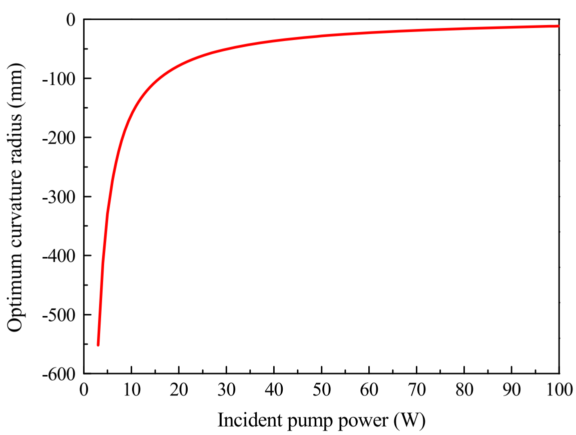

Fig. 3. Optimum curvature of the mirror M1 versus the incident pump power.

stability of cavity. Calculative result shows that $R_1=-100$ mm and $R_1=-50$ mm fit to the pump region of 15–60 W and 30–70 W, respectively. Compared with plano–plano cavity, the lasing threshold of the unstable cavity is increased, but it is propitious to high pump power. As a result, M_1 with curvature of -100 mm is used in experiments to realize high power pulsed laser operation; then a good mode-matching is also obtained.

3.2. Fundamental-wave operation

For improving the output power of A-O Q-switched 912 nm laser, tests are conducted to estimate the best transmissivity of output coupling mirror (M_2). The output characteristics of pulsed 912 nm laser are measured as the M_2 has a transmissivity of $T=6\%$, 9% and 12% at 912 nm. As shown in Fig. 4, it can be seen that M_2 with $T=9\%$ is favorable of achieving high power pulsed 912 nm laser output. The lasing threshold is 20.8 W and the maximum average output power of 2.3 W is obtained at an incident pump power of 49.5 W, corresponding to an optical conversion efficiency of 4.6% and an average slope efficiency of 9.2%. If the low absorption efficiency of the pump radiation ($\eta_\alpha=60\%$) was taken into account, the slope efficiency could be up to 15.3% with respect to the absorbed pump power.

At 10 kHz, the pulse width and peak power of 912 nm laser as a function of the incident pump power are presented in Fig. 5. It can be seen that, when the incident pump power is lower than 45.3 W, the pulse width is reduced and the peak power is increased exponentially with the increase of the incident pump power. At an incident pump power of 45.3 W, a minimum pulse width of

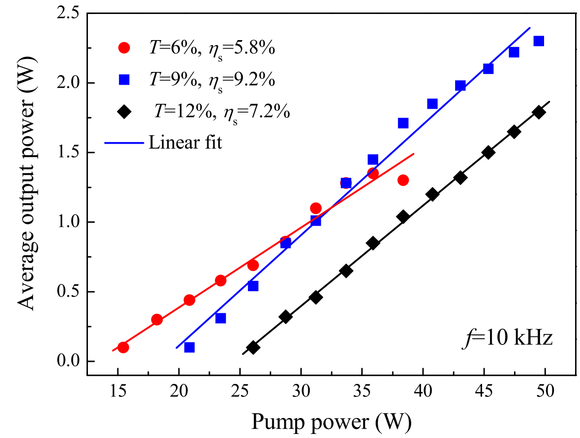

Fig. 4. Average output power of 912 nm laser versus incident pump power at 10 kHz.

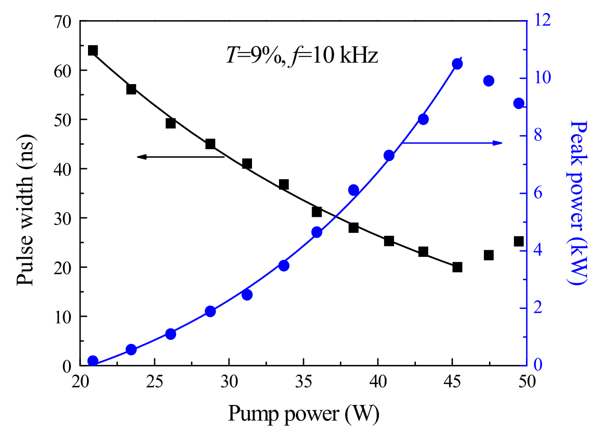

Fig. 5. Pulse width and peak power of 912 nm laser versus incident pump power at 10 kHz.

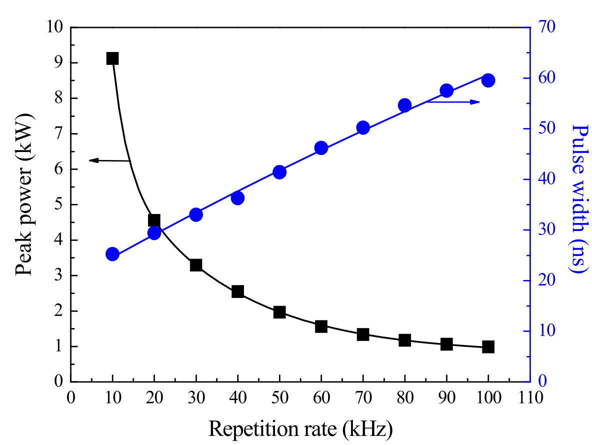

Fig. 6. Peak power and pulse width of 912 nm laser versus the repetition rate.

20 ns 912 nm laser is obtained, with the highest peak power of 10.5 kW. With the increase of the pump power, the pulse width increases and the peak power reduces; this is attributed to the deterioration of the laser beam quality resulting from thermal effect. At an incident pump power of 49.5 W, the pulse width is 25.2 ns.

At the incident pump power of 49.5 W, the 912 nm laser performance at different repetition rates (10–100 kHz) is investigated and depicted in Fig. 6. With the increase of the repetition rate, the pulse width is increased and the peak power is decreased.

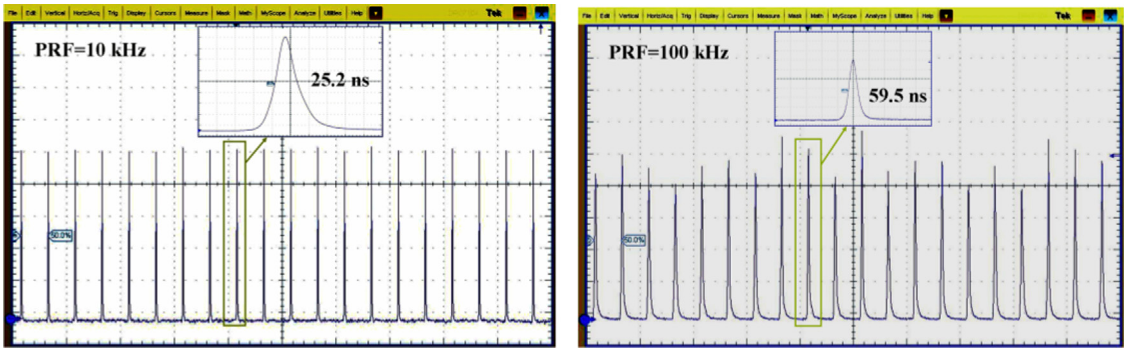

Fig. 7. Pulse trains and typical shapes of the 912 nm laser at 10 kHz and 100 kHz.

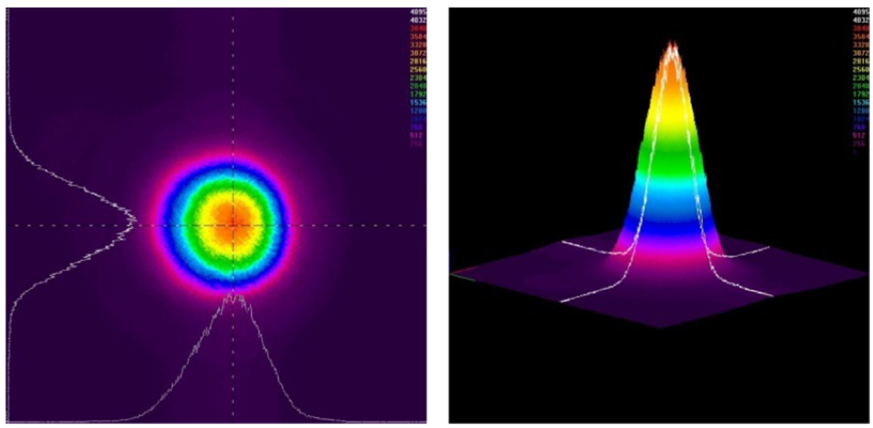

Fig. 8. Laser intensity profile of the 2.3 W 912 nm laser.

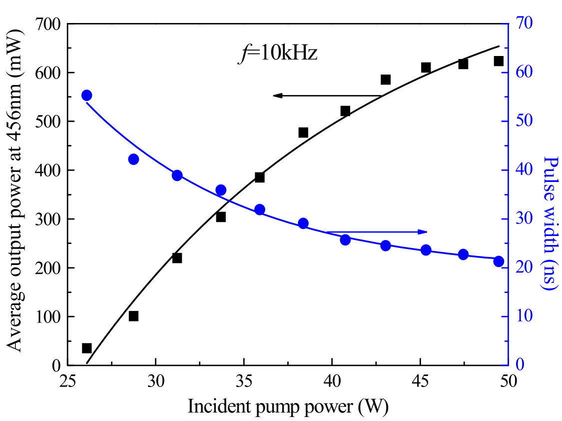

Fig. 9. Average output power and pulse width of 456 nm light versus pump power at 10 kHz.

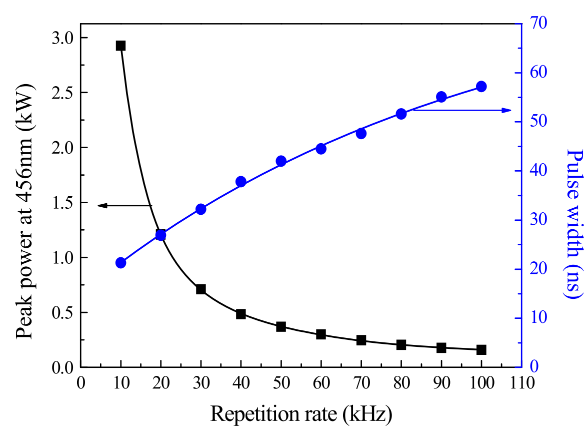

Fig. 10. Peak power and pulse width of 456 nm light versus repetition rate.

At 100 kHz, the pulse width is increased to 59.5 ns and the peak power is reduced to 0.99 kW. Pulse trains and typical pulse shapes of 912 nm laser at 10 kHz and 100 kHz are shown in Fig. 7. It can be seen that the pulse amplitudes jitter at 100 kHz operation, which indicates that the laser gain is not enough to satisfy a stable high-repetition-rate operation, but no loss of pulse is observed if the operating duty cycle for Q-switch is chosen properly.

The 2-D and 3-D far field laser beam intensity profile of 912 nm laser at the maximum average output power of 2.3 W recorded by a laser beam analyzer (LBA-712PC-D, Spiricon Inc.) is shown in Fig. 8. It can be seen that the laser intensity distribution is very symmetrical and near Gaussian-distribution. Beam quality is measured by using a traveling knife-edge method, and it is estimated to be $M_x^2=1.35$ and $M_y^2=1.28$.

3.3. Second-harmonic generation

Extra-cavity frequency doubling structure is designed as shown in Fig. 1. To improve the conversion efficiency during secondary harmonic generation, the 912 laser is focused into the nonlinear crystal by a lens (lens1: $f=50$ mm). Distance between lens1 and M_2, M_3 and lens1, M_4 and M_3 is 120 mm, 25 mm and 85 mm, respectively. BiBO crystal is put near M_4 for a beam waist $\sim$90 μm is generated.

The average output power and pulse width of 456 nm deep-blue light versus pump power at 10 kHz is shown in Fig. 9. With the increase of pump power, the output power and pulse width is increased and reduced exponentially, respectively. At the incident pump power of 49.5 W, the average output power of the 456 nm light is 623 mW, with a pulse width of 21.3 ns. Peak power and pulse width of 456 nm light versus repetition rate are shown in Fig. 10, and with the increase of repetition rate, the peak power and pulse width are reduced and increased exponentially. From 10 kHz to 100 kHz, the peak power is reduced from 2.3 kW to 0.16 kW, and the pulse width is increased from 21.3 ns to 57.2 ns.

4. Conclusion

A diode-pumped A-O Q-switched 912 nm $Nd:GdVO_4$ laser and 456 nm deep-blue light by extra-cavity frequency-doubling are demonstrated in this paper. Using a compact thermal-compensating laser cavity with a $T=9\%$ output coupler, a maximum average output power of 2.3 W 912 nm laser is obtained at 10 kHz, giving an optical conversion efficiency of 4.6% and a slope efficiency of 9.6%. A minimum pulse width of 20 ns and a maximum peak power of 10.5 kW are achieved at a pump power of 45.3 W. Employing a BiBO crystal as frequency-doubler, maximum average output power of 623 mW 456 nm deep-blue light is obtained at 10 kHz, with a pulse width of 21.3 ns and a peak power of 2.3 kW. Stable operating repetition rate for 912 nm laser and 456 nm light can be extended to 100 kHz.

Acknowledgments

We gratefully acknowledge support from the National Natural Science Foundation of China (Grant no. 61308050) and the Fundamental Research Project of Chinese State Key Laboratory of Laser Interaction with Matter (Grant nos. SKLLIM 1210-01 and SKLLIM 1210-02).

References

[1] Castaing M, Balembois F, Georges P, Georges T, Schaffers K, Tassano J. Diode-pumped $Nd:YVO_4$/Yb:S-FAP laser emitting at 985 and 492.5 nm. Opt Lett 2008;33:1234–6.
[2] Shi Z, Fan Z, Wang P, Zhang J, Niu G, Cui J. High efficiency continuous-wave laser-diode-end-pumped vanadate laser operating on 914 nm. Chin J Lasers 2008;35:329–32 (in Chinese).
[3] Chen F, Yu X, Gao J, Li X, Yan R, Yu J, et al. 8.9-W continuous-wave, diode-end-pumped all-solid-state $Nd:YVO_4$ laser operating at 914 nm. Laser Phys. 2009;19:389–91.
[4] Matioli E, Brinkley S, Kelchner K, Hu Y, Nakamura S, DenBaars S, et al. High-brightness polarized light-emitting diodes. Light: Sci Appl 2012;1:e122.
[5] Limpert J, Stutzki F, Jansen F, Otto H, Eidam T, Jauregui C, et al. Yb-doped large-pitch fibers: effective single-mode operation based on higher-order mode delocalization. Light: Sci Appl 2012;1:e8.
[6] Yokozawa T, Nakajima H, Yamamoto T, Hara H. Oscillation characteristics of diode-pumped Tm:YAG and Tm, Ho:YAG microchip lasers. Rev Sci Instrum 1995;66:4453–7.
[7] Czeranowsky C, Heumann E, Huber G. All-solid-state continuous-wave frequency-doubled Nd:YAG-BiBO laser with 2.8-W output power at 473 nm. Opt Lett 2003;28:432–4.
[8] Buryy O, Sugak D, Ubizskii S, Izhnin I, Vakiv M, Solskii I. The comparative analysis and optimization of the free-running Tm^{3+}:YAP and Tm^{3+}:YAG microlasers. Appl Phys B 2007;88:433–42.
[9] Dianov E. Bismuth-doped optical fibers: a challenging active medium for near-IR lasers and optical amplifiers. Light: Sci Appl 2012;1:e12.
[10] Pincella F, Isozaki K, Miki K. A visible light-driven plasmonic photocatalyst. Light: Sci Appl 2014;3:e133.
[11] Fan T, Byer R. Model and CW operation of a quasi-three-level 946 nm Nd:YAG laser. IEEE J Quantum Electron 1987;23:605–12.
[12] Zhou R, Li E, Li H, Wang P, Yao J. Continuous-wave, 15.2 W diode-end-pumped Nd:YAG laser operating at 946 nm. Opt Lett 2006;31:1869–71.
[13] Krennrich D, Knappe R, Henrich B, Wallenstein R, L'huillier J. A comprehensive study of Nd:YAG, $NdYAlO_3$, $Nd:YVO_4$ and $Nd:YGdVO_4$ lasers operating at wavelengths of 0.9 and 1.3 μm. Part 1: cw-operation. Appl Phys B 2008;92:165–74.
[14] Yu X, Wang C, Chen F, Yan R, Li X, Peng J, et al. High repetition rate, high peak power acousto-optical Q-switched 946 nm Nd:YAG laser. Laser Phys 2010;20:1783–6.
[15] Yu X, Chen F, Yan R, Li X, Yu J, Zhang Z. High power diode-pumped 914-nm $Nd:YVO_4$ laser. Chin Opt Lett 2010;8:499–501.
[16] Zhang C, Zhang L, Wei Z, Zhang C, Long Y, Zhang Z, et al. Diode-pumped continuous-wave $Nd:LuVO_4$ laser operating at 916 nm. Opt Lett 2006;31:1435–7.
[17] Zhang L, Zhang C, Wei Z, Zhang Z, Strohmaier S, Eichler H. Characteristics of $Nd:GdVO_4$ laser with different Nd-doping concentrations. Chin Phys Lett 2006;23:2088–91.
[18] Gao J, Yu X, Chen F, Li X, Yan R, Zhang K, et al. 12.0-W continuous-wave diode-end-pumped $Nd:GdVO_4$ laser with high brightness operating at 912-nm. Opt Express 2009;17:3574–80.
[19] Gong W, Qi Y, Bi Y. A comparative study of continuous laser operation on the $^4F_{3/2}$–$^4I_{9/2}$ transitions of $Nd:GdVO_4$ and $Nd:YVO_4$ crystals. Opt Commun 2009;282:955–7.
[20] Yu X, Chen F, Yan R, Li X, Yu J, Zhang Z. 912 nm laser operation in diode-pumped grown-together composite $Nd:GdVO_4/GdVO_4$ crystal. Laser Phys 2009;19:1–5.
[21] Chen F, Yu X, Li X, Yan R, Wang C, Luo M, et al. Theoretical and experimental investigations of a diode-pumped high-power continuous-wave 912 nm $Nd:GdVO_4$ laser operation at room temperature. Opt Commun 2010;283:3755–60.
[22] Zheng Q, Yao Y, Li B, Zhou K, Liu Y, Zhao L. Experimental study of the generation of a blue laser by intracavity frequency doubling of a cw $Nd:GdVO_4$ laser with lithium borate. Appl Opt 2009;48:2979–82.
[23] Yan R, Yu X, Chen D, Chen F, Li X, Ma Y, et al. Improved performance of diode-end-pumped $Nd:GdVO_4$ 912 nm laser property with indium solder technology. Laser Phys 2011;21:462–7.
[24] Hong H, Liu Q, Liu H, Fu X, Gong M. $Nd:GdVO_4$ slab laser with line-shaped end-pumping profile operating at 912 nm. Laser Phys 2011;21:855–60.
[25] Chen F, Yu X, Wang C, Yan R, Li X, Gao J, et al. Passively Q-switched 912 nm $Nd:GdVO_4$/Cr:YAG laser at high repetition rate operation. Laser Phys 2010;20:1275–8.
[26] Chen F, Yu X, Li X, Yan R, Wang C, Luo M, et al. Diode-pumped passively Q-switched 912 nm $Nd:GdVO_4$ laser and pulsed deep-blue laser by intracavity frequency-doubling. Opt Commun 2010;283:4036–40.
[27] Xu C, Wei Z, He K, Li D, Zhang Y, Zhang Z. Diode-pumped passively mode-locked $Nd:GdVO_4$ laser at 912 nm. Opt Commun 2008;281:4398–400.
[28] Chen F, Yu X, Li X, Yan R, Wang C, Chen D, et al. High power diode-pumped passively Q-switched and mode-locking $Nd:GdVO_4$ laser at 912 nm. Opt Commun 2011;284:635–9.
[29] Gao J, Yu X, Chen F, Li X, Zhang Z, Yu J, et al. Characteristics of CW and A-O Q-switched $Nd:GdVO_4$ laser operation at 912 nm. Advanced solid-state photonics. Technical Digest (Optical Society of America; 2008 (paper WB7).
[30] Gao J, Yu X, Chen F, Li X, Yan R, Zhang Z, et al. Pulsed 456 nm deep-blue light generation by acousto-optical Q-switching and intracavity frequency doubling of $Nd:GdVO_4$. Laser Phys Lett 2008;5:577–81.
[31] Zang Z, Minato T, Navaretti P, Hinokuma Y, Duelk M, Velez C, et al. High-power (> 110 mW) superluminescent diodes by using active multimode interferometer. IEEE Photon Technol Lett 2010;22:721–3.
[32] Zang Z, Mukai K, Navaretti P, Duelk M, Velez C, Hamamoto K. Thermal resistance reduction in high power superluminescent diodes by using active multi-mode interferometer. Appl Phys Lett 2012;100:031108.
[33] Yan R, Yu X, Li X, Chen D, Gao J. Study of the thermal effect in $Nd:GdVO_4$ 912 nm CW laser. J Russ Laser Res 2013;34:114–9.